



Different rates of endocytic activity and vesicle transport from the apical and synaptic poles of the outer hair cell

Hair cells in the sensory epithelium of the cochlea are vulnerable and do not regenerate spontaneously. Therefore, ideally, the cells must function for the entire lifetime of the mammal. However, there is still little known about the membrane- and protein-recycling machinery of hair cells. The present study investigates endocytosis and vesicle trafficking of outer hair cells using fluorescent membrane markers. Understanding of the underlying mechanisms is a prerequisite for the future design of cell-specific medication for hair-cell rehabilitation or regeneration.

Introduction

Outer hair cells (OHCs)—the electromotile elements of the organ of Corti—are responsible for the high-frequency selectivity as well as low-threshold and broad dynamic range of hearing [2, 6, 20]. In response to a change of transmembrane potential, they produce an electromechanical force of up to at least 50 kHz [10], which acts against frictional forces [8], resulting in the intensity-dependent frequency tuning and amplitude gain of the vibration response of the organ of Corti. The apical pole of the OHC is the site of mechano-electrical transduction, where hair-bundle deflection causes ion influx accompa-

nied by a change of the transmembrane potential [9]. The basal pole is the place of synaptic communication with nerve fibers from the efferent and afferent systems. The (medial) efferents modulate the electromechanical response of the OHC via calcium-activated changes of the transmembrane potential and cell stiffness [17], which result in a conformation change of the electromotile protein, prestin [35], expressed in high density in the lateral plasma membrane (PM) of the OHC [19], as well as modulation of the electromechanical force produced by the cell. The (type II) afferents are the source of a feedback signal to the soma of the medial efferents in the brainstem [11].

Although cochlear hair cells are functionally vulnerable and not capable of spontaneous regeneration and, hence, required for the entire lifetime of the mammal, there is still little known about the membrane- and protein-recycling machinery driven by endo- and exocytosis. Different types of vesicles have been demonstrated at the apical and basal poles of OHCs [21, 27]. Investigations of the dynamics of membrane recycling using PM fluorescent labeling and confocal microscopy revealed rapid apical endocytic activity and intracellular vesicle trafficking in OHCs [16, 25]. Endocytosis has been proposed to be involved in gentamicin uptake by hair cells and accessory epithelia of the organ of Corti [7]. The development of cell-specific medication to treat sensorineural hearing loss will rely not only on investigations of

drug delivery to specific targets within the cochlea [29], but also on an understanding of fundamental cellular internalization processes such as endocytic activity and vesicle trafficking.

Here, we investigate the spatial and temporal properties of endocytic internalization and transport of fluorescent membrane markers applied to OHCs isolated from the guinea pig cochlea. Using a newly developed double-barrel perfusor to apply the markers separately to the basal and apical halves of the OHC [18], we demonstrate greater endocytic uptake in the synaptic region and faster vesicle trafficking in the basoapical direction.

Methods

Cell isolation

Outer hair cells were isolated and handled as previously described [18]. Adult pigmented guinea pigs with a weight of 350–900 g ($N=21$) were used for the study. The data derive from 37 cells isolated from 21 cochleae. Animals were anesthetized by intraperitoneal injection of a mixture of 100 mg/kg ketamine and 4 mg/kg xylazine and were killed by cervical dislocation. The dissected temporal bones were placed in an ice-chilled Hanks' balanced salt solution (HBSS; Biochrom KG, Berlin, Germany), containing: 137 mM NaCl, 5.4 mM KCl, 1.25 mM CaCl₂, 4.2 mM NaHCO₃, 0.81 mM MgSO₄·7H₂O, 0.44 mM KH₂PO₄, 0.34 mM

These data were presented at the 55th Inner Ear Biology Workshop, held in Berlin in September 2018.

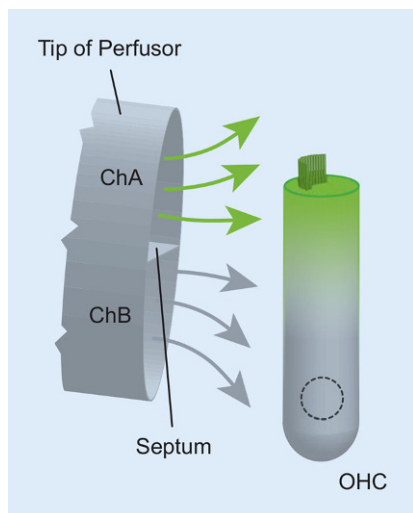


Fig. 1 ▲ Local perfusion using a double-barrel perfusor. The tip of the double-barrel perfusor is positioned close to the basolateral plasma membrane of the isolated outer hair cell (OHC). The septum separates channel A (ChA) and channel B (ChB). In this example, HBSS containing green dye is applied from ChA to the apical pole of the cell and dye-free HBSS from ChB to the basal pole. This stimulus configuration allows *apicobasal* vesicle trafficking to be studied; conversely, swapping the channels allows *basoapical* trafficking to be studied. Channels are connected to a peristaltic pump to drive the channels in parallel at a speed that ensures laminar flow around the cell

$\text{Na}_2\text{HPO}_4 \cdot 2\text{H}_2\text{O}$, 5 mM glucose, and 5 mM HEPES, with an osmolarity of 310 mOsm/l adjusted with D-(+)-glucose; the pH was 7.3. HBSS was used as the extracellular fluid throughout the preparation steps and experiments. All chemicals were from MERCK (Darmstadt, Germany), unless otherwise stated. Outer hair cells from the apical third of the cochlea were isolated; their lengths were $74 \pm 7 \mu\text{m}$.

Perfusion systems

Single- or double-barrel perfusors (■ Fig. 1) were used, respectively, to label either both poles or a single pole of the OHC [18]. The tip of the perfusor was positioned near the cell using a micromanipulator (SM5, Luigs and Neumann GmbH, Ratingen, Germany). A peristaltic pump (Ismatec, IDEX Health & Science GmbH, Wertheim, Germany) established laminar flow with a constant flow rate.

Using a single-barrel perfusor enabled homogeneous labeling of the entire PM; the flow rate was $14 \mu\text{l}/\text{min}$. By contrast, using a double-barrel perfusor enabled labeling of a single pole of the OHC (■ Fig. 1). The double-barrel perfusor was fabricated from a borosilicate-glass theta capillary with an external diameter of 2 mm (Harvard Apparatus, MA, USA) using a DMZ-Universal Puller (Zeitz Instruments, Augsburg, Germany). To achieve single-pole staining, the perfusor tip was positioned as close as possible to the cell. The coverslip was coated with a cell-and-tissue adhesive (Cell-Tak™) to facilitate cell adhesion. The output flow rate was $3 \mu\text{l}/\text{min}$ per barrel. As recently demonstrated [18], the double-barrel perfusion method is an effective tool for exclusively labeling one pole of bipolar cells such as OHCs.

Fluorescence microscopy

Imaging was performed using a Zeiss LSM 510 confocal laser-scanning system based on a Zeiss Axioskop2 FS mot microscope (Zeiss, Heidelberg, Germany) equipped with a two-photon laser system (Mira™ 900 Ti:Sapphire Laser pumped by a Verdi V5 Diode-Pumped Laser from Coherent, Santa Clara, USA) and a pin-hole diameter of 1 AU. A Zeiss $40 \times$ IR-Achroplan water-immersion objective with NA 0.8 and ZEN2009 software was used.

The fluorescent membrane markers FM1-43 [N-(3-triethylammoniumpropyl)-4-(4-(dibutylamino)styryl)pyridinium dibromide] and FM4-64 [N-(3-triethylammoniumpropyl)-4-(6-(4-(diethylamino)phenyl)hexatrienyl)pyridinium dibromide] were used to visualize endocytosis. FM1-43 is a green-fluorescent, lipophilic styrylpyridinium dye that is commonly used to visualize endocytic and exocytic processes [3], also in cochlear hair cells [15, 16, 18, 23]. Virtually non-fluorescent in aqueous media, the dye rapidly inserts into the PM where it becomes intensely fluorescent; excitation/emission spectral maxima are $473/579 \text{ nm}$, respectively. FM4-64 is a derivative of FM1-43 with similar membrane labeling properties, but exhibits longer wavelength (red) flu-

orescence making it suitable for double-labeling experiments with lower wavelength dyes [18]; the excitation/emission spectral maxima are $505/725 \text{ nm}$, respectively. Stock solutions of these dyes in a concentration of 10 mM were prepared in DMSO. On the day of the experiment, the dyes were diluted in HBSS to a final concentration of $10 \mu\text{M}$.

The fluorescent endoplasmic marker DiOC₆ (3,3'-dihexyloxycarbocyanine iodide) was used to examine possible targets of endocytosed vesicles in the endoplasmic reticulum (ER). DiOC₆ is a cell-permeant, green-fluorescent, lipophilic dye, which at low concentrations is selective for mitochondria of live cells and at high concentrations labels other intracellular structures, such as ER [24, 34]. Excitation/emission spectral maxima are $489/506 \text{ nm}$, respectively. For double-labeling experiments with FM4-64 and DiOC₆, OHCs were first incubated in DiOC₆ for 1 min, the DiOC₆ was washed out with extracellular solution, and then the FM4-64 was applied. This FM dye was used instead of FM1-43 because the fluorescence spectra of FM4-64 and DiOC₆ can be readily separated using bandpass filters. A 1-mg/ml stock solution of DiOC₆ was prepared in DMSO. Just before the experiments began, it was diluted with HBSS to a final concentration of $0.87 \mu\text{M}$ [23].

The fluorescent fluid-phase marker Lucifer yellow (Lucifer yellow carbohydrazide, potassium salt) was used to examine pinocytosis. Lucifer yellow is a well-known dye for studying fluid-phase endocytosis [15]. The dye is hydrophilic, but being anionic cannot permeate the cell membrane by passive diffusion. The potassium-salt of Lucifer yellow has excitation/emission spectral maxima at $428/536 \text{ nm}$, respectively. A 50-mM stock solution of Lucifer yellow was prepared in DMSO. On the day of the experiments, it was diluted with HBSS to a final concentration of $50 \mu\text{M}$. This concentration was chosen to be of the same order of magnitude as that of the FM dyes ($10 \mu\text{M}$).

FM and DiOC₆ were excited with an argon laser with a wavelength of 488 nm and the emitted light was collected with bandpass filters: $505\text{--}750 \text{ nm}$ for

HNO 2019 · 67:449–457 <https://doi.org/10.1007/s00106-019-0674-y>
© The Author(s) 2019

C. Harasztosi · A. W. Gummer

Different rates of endocytic activity and vesicle transport from the apical and synaptic poles of the outer hair cell

Abstract

Background. Intense endocytic activity at the apex of outer hair cells (OHCs)—the electromechanical cells of the cochlea—has been demonstrated using the vital plasma-membrane marker FM1-43 and confocal laser-scanning microscopy. Vesicular traffic toward the cell nucleus to distinct locations of the endoplasmic reticulum has also been shown.

Objective. The current study characterizes the dynamics of endocytic activity, as well as apicobasal and basoapical trafficking, using a local perfusion technique that we recently developed and published to visualize bidirectional trafficking in isolated bipolar cells.

Materials and methods. The fluorescent plasma-membrane markers FM1-43 (10 μM) and FM4-64 (10 μM), together with a fluid-phase marker, Lucifer yellow (50 μM), were used to label endocytosed vesicles in isolated OHCs of the guinea pig cochlea. Targets of endocytosed vesicles were examined with a fluorescent marker of subsurface cisternae, DiOC₆ (0.87 μM). Single- and two-photon confocal laser-scanning microscopy was used to visualize labeled vesicles.

Results. The plasma-membrane markers presented more intense vesicle internalization at the synaptic pole than at the apical pole of the OHC. Intracellular basoapical vesicle

trafficking was faster than apicobasal trafficking. Vesicles endocytosed at the synaptic pole were transcytosed to the endoplasmic reticulum system. An intracellular Lucifer yellow signal was not detected.

Conclusion. The larger endocytic fluorescent signals in the synaptic pole and the faster basoapical trafficking imply that membrane internalization and vesicle trafficking are more efficient at the synaptic pole than at the apical pole of the OHC.

Keywords

Cochlea · Endocytosis · Pinocytosis · Transcytosis · FM dyes

Unterschiedliche Raten von endozytischer Aktivität und Vesikeltransport am apikalen und synaptischen Pol der äußeren Haarsinneszelle

Zusammenfassung

Hintergrund. Intensive endozytische Aktivität am apikalen Pol der äußeren Haarsinneszelle (ÄHZ) – der elektromechanischen Zelle der Cochlea – wurde mit dem vitalen Plasmamembranmarker FM1-43 unter Einsatz konfokaler Laserscanningmikroskopie nachgewiesen. Es wurde gezeigt, dass Vesikel in Richtung Zellkern zu unterschiedlichen Bereichen des endoplasmatischen Retikulums (ER) transportiert werden.

Fragestellung. Ziel der aktuellen Studie war es, die Dynamik der endozytischen Aktivität sowie des apikobasalen und basoapikalen Vesikeltransports mittels einer vor Kurzem von den Autoren entwickelten lokalen Perfusionstechnik zu charakterisieren, welche die Visualisierung von bidirektionalem

Vesikeltransport in isolierten bipolaren Zellen ermöglicht.

Material und Methode. Die fluoreszierenden Plasmamembranmarker FM1-43 (10 μM) und FM4-64 (10 μM) sowie der fluoreszierende Fluidphasenmarker Lucifer Yellow (50 μM) wurden verwendet, um endozytierte Vesikel in isolierten ÄHZ der Meerschweinchencochlea zu markieren. Ziele der endozytierten Vesikel wurden mit einem ER-Fluoreszenzmarker, DiOC₆ (0,87 μM), untersucht. Fluoreszierende Vesikel wurden mittels Einzel- und Zwei-Photonen-Laserscanningmikroskopie sichtbar gemacht.

Ergebnisse. Die Plasmamembranmarker zeigten eine intensivere Vesikelaufnahme am synaptischen als am apikalen Pol der ÄHZ. Der

intrazelluläre Vesikeltransport in basoapikaler Richtung war schneller als in apikobasaler Richtung. Am synaptischen Pol endozytierte Vesikel wurden zum ER transportiert. Ein intrazelluläres fluoreszierendes „Lucifer-Yellow-Signal“ wurde nicht detektiert.

Schlussfolgerungen. Die intensiveren endozytischen Fluoreszenzsignale im synaptischen Pol und der schnellere Transport in die basoapikale Richtung deuten darauf hin, dass Membranaufnahme und Vesikeltransport effizienter am synaptischen als am apikalen Pol der ÄHZ sind.

Schlüsselwörter

Cochlea · Endozytose · Pinozytose · Transzytose · FM-Farbstoffe

FM1-43, 650–710 nm for FM4-64, and 500–550 nm for DiOC₆. For the double-labeling experiments with FM4-64 and DiOC₆, the emitted light was separated into two channels using a dichroic beam splitter (NFT545). Lucifer yellow was excited by the two-photon laser (840 nm) and the emission recorded below 650 nm using a short-pass filter (KP650).

Except for the Lucifer yellow experiments, fluorescence signals were corrected offline for the average background fluorescence level, which was measured

extracellularly just before the start of dye application in a region free of cell remnants.

All dyes were purchased from Thermo Fisher Scientific, Inc. (Waltham, MA, USA).

Data analysis

The detection threshold, used for calculating signal delay, was set to 20% of the saturation intensity from the PM region of interest (ROI) near the cell pole where

the dye was applied. Linear regression, with software in Origin (Ver. 7, OriginLab Corporation, Northampton, MA, USA), was used to estimate the time at which the signal reached/crossed the 20% value. Linear regression was also used for calculating the mean speed of vesicle trafficking. Average data are presented as mean and standard deviation. Statistical tests were performed with the Student's *t* test and considered significant at $p < 0.05$. Test results are given as *p* and *t_f* values, where *f* denotes the degrees of freedom.

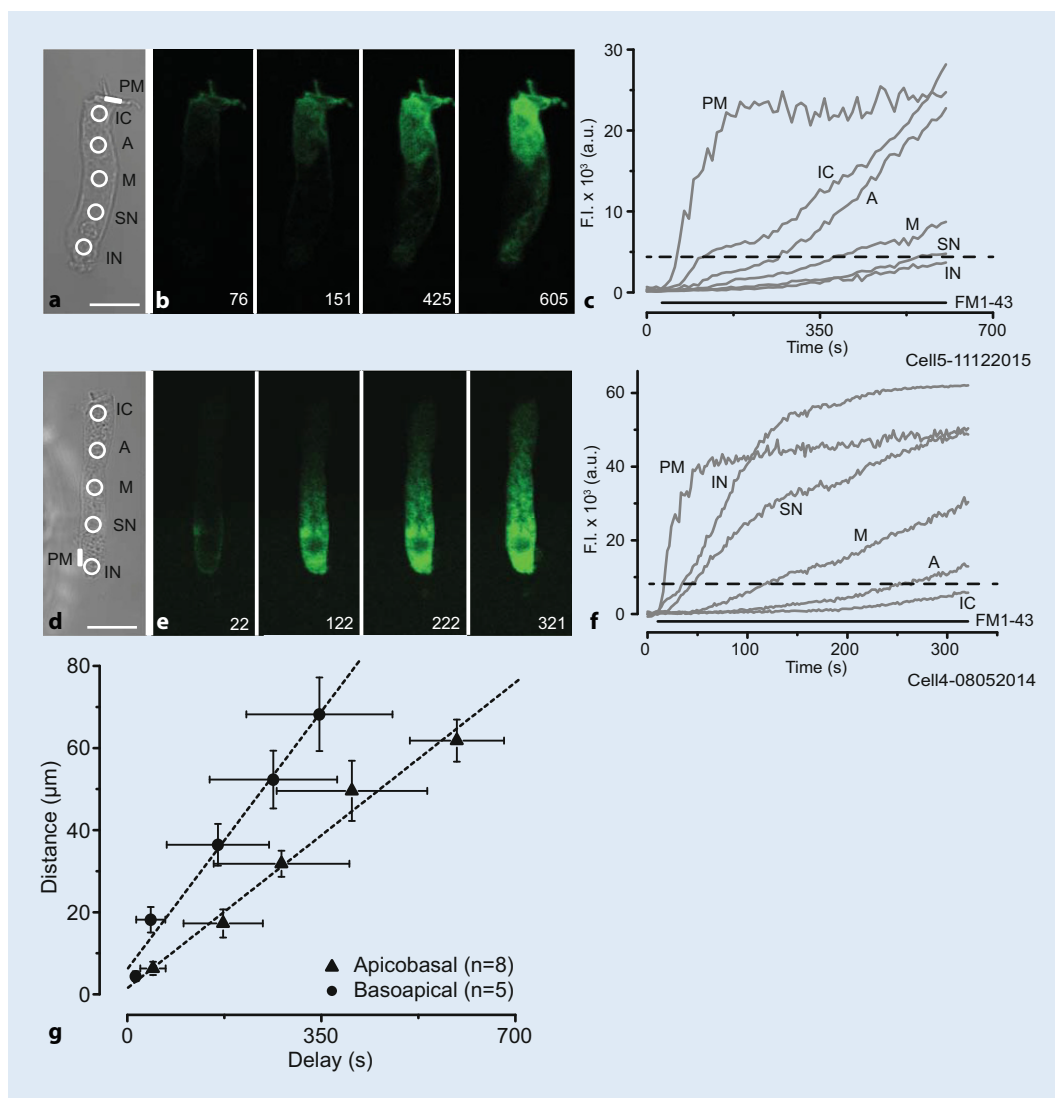


Fig. 2 ▲ Uptake and trafficking of FM1-43 applied to the apical or basal region of the isolated OHC. **a–c** Apical labeling and apicobasal trafficking. **d–f** Basal labeling and basoapical trafficking. Data are from different cells. **a, d** Phase-contrast images showing the regions of interest (ROIs) used for analysis (circles and the rectangle): IC infracuticular, A apical, M middle, SN supranuclear, IN infranuclear, PM plasma membrane. Scale bar: 20 μm. The tip of the double-barrel capillary is positioned near the cell from the left side (not shown). **b, e** Fluorescence images showing the spatial and temporal courses of cell labeling. Numbers in the bottom right corners indicate experimental time in seconds. **c, f** Fluorescence signal intensities calculated from the ROIs in panel **a** and **d**, respectively. Dashed black line: 20% of the steady-state signal level in the PM ROI, used to estimate the signal delay to a given ROI relative to the PM ROI. Horizontal black line: FM1-43 application period. **g** Average distance of ROIs from a cell pole as function of time delays of the ROIs relative to the PM ROI for apicobasal (8 cells) and basoapical (5 cells) vesicle traffic. Error bars: standard deviations. Dashed lines: linear regression lines used to estimate trafficking speed

Results

Apicobasal and basoapical trafficking

Endocytic activity was investigated separately at the apical and basal poles of the isolated OHC (Fig. 2). In the first example shown (Fig. 2a–c), the PM marker FM1-43 was applied to the apical pole of the OHC using the dou-

ble-barrel perfusor (Fig. 2a). Channel A (ChA) contained 10 μM FM1-43 in HBSS while channel B (ChB) contained dye-free HBSS to prevent apical pole labeling. The spatial distribution and the temporal course of the intracellular dye (Fig. 2b) imply that FM-labeled vesicles traffic toward the base of the cell. Fig. 2c shows the time course of the fluorescence signal intensities in the ROIs indicated in Fig. 2a. The dashed line

denotes 20% of the saturation intensity from the apically located PM ROI. This 20% value, arbitrarily set as a threshold signal value, was used to calculate the signal delays to the ROIs relative to the PM ROI. Distances of the ROIs from the apical pole are plotted as a function of signal delay in Fig. 2g (triangles) for the average of eight cells. Based on linear regression, the slope yields an average apicobasal speed of $0.11 \pm 0.01 \mu\text{m/s}$. The

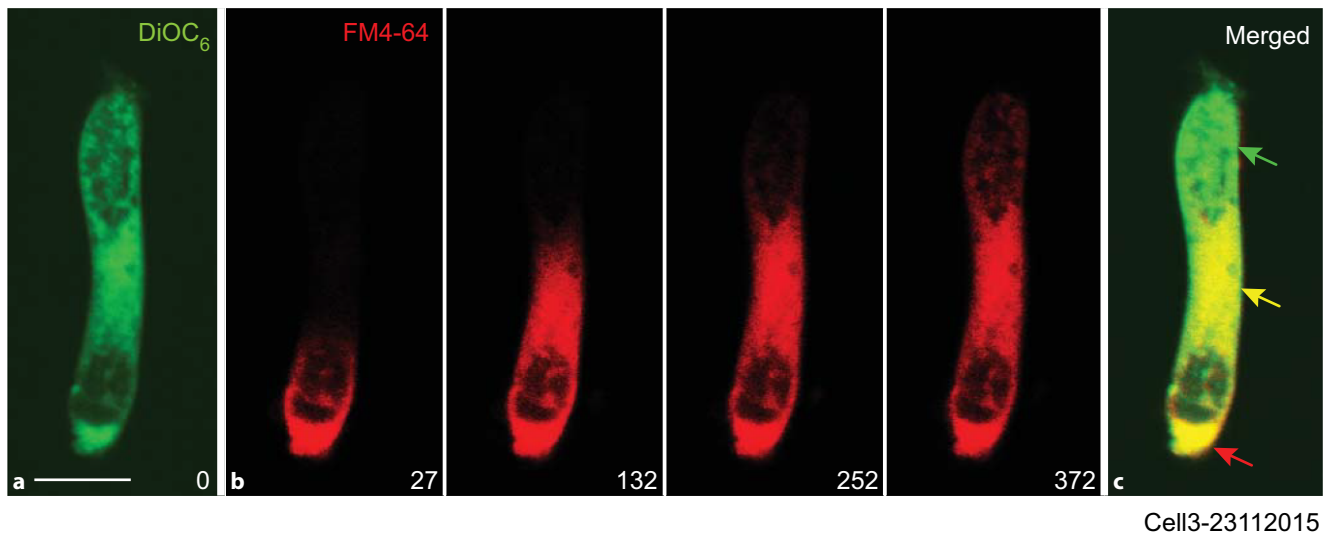


Fig. 3 ▲ Targets of basal endocytosed vesicles. **a** Endoplasmic reticulum of an outer hair cell labeled with DiOC₆ (0.87 μM). The image was taken after a 1-min incubation in the dye. *Scale bar:* 20 μM. **b** Spatial and temporal courses of fluorescent vesicles of FM4-64 (10 μM) for dye application at the basal pole. *Numbers in the bottom right corners* indicate experimental time in seconds. **c** Image of panel **a** merged with the last image in panel **b**, the yellow staining demonstrating colocalization of DiOC₆ and FM4-64 labeling

distance–axis intercept locates the PM ROI, on average, at $1.52 \pm 3.09 \mu\text{m}$ from the apical pole, which is not significantly different from $0 \mu\text{m}$ ($t_7 = 1.39$, $p = 0.21$).

The same protocol was used to investigate basoapical trafficking, the FM1-43 dye being applied to the basal half of the cell (ChB) and the dye-free HBSS to the apical half (ChA) to prevent access of dye to that region (■ Fig. 2d–f). Signal delay as a function of distance from the basal pole is shown in ■ Fig. 2g (circles) for five cells. The average apicobasal speed is $0.18 \pm 0.01 \mu\text{m/s}$. The distance–axis intercept locates the PM ROI, on average, at $6.25 \pm 2.73 \mu\text{m}$ from the basal pole. In other words, the basoapical speed is significantly greater than the apicobasal speed ($t_6 = 12.17$, $p = 9.37 \cdot 10^{-6}$), indicating more intense trafficking toward the apex of the cell.

For the apical application, the fluorescent signal in the infranuclear ROI required, on average, $45.1 \pm 22.8 \text{ s}$ ($N = 8$) to reach the 20% threshold, whereas for the basal application, on average, only $13.6 \pm 6.4 \text{ s}$ ($N = 5$) was required for the infranuclear ROI, relative to the respective PM ROIs at or near the poles. The significantly smaller delay for the infranuclear ROI ($t_{11} = 3.44$, $p = 0.003$) indicates that vesicle formation in the synaptic pole is

more intense than that at the apex of the OHC.

Targets of basal endocytosed vesicles

Until now, targets of vesicles formed at the synaptic pole of OHCs had not been demonstrated. Therefore, here, the endoplasmic reticulum of OHCs was labeled with DiOC₆ (■ Fig. 3a, green) and compared with vesicle targets of the fluorescence PM marker FM4-64 applied to the basal pole (■ Fig. 3b, red). The yellow signal in ■ Fig. 3c indicates colocalization of DiOC₆ and FM4-64. Similar observations were made in a total of 14 cells. These observations imply that basally endocytosed vesicles are transcytosed to the endoplasmic reticulum.

Molecular weight limit of endocytosed molecules

To investigate the maximum possible molecular weight (MW) for a substance to be internalized by fluid-phase endocytosis (pinocytosis), Lucifer yellow (MW = 522 Da) was applied to the OHC and the development of intracellular fluorescence recorded (■ Fig. 4). In these experiments ($N = 10$), a single-barrel perfusor was used to apply the stain ho-

mogeneously around the entire cell. To avoid recording of scattered emitted light from extracellular dye, fluorescence was induced and recorded with two-photon confocal microscopy. Despite the presence of a constant and high-intensity extracellular signal and an extensive application time of the dye (>30 min), an intracellular fluorescence signal was not detected above the background noise level (■ Fig. 4). Importantly, the displayed intracellular signals represent noise derived from the extracellular signal because the intracellular signal dropped to zero when the Lucifer yellow application was terminated and extracellular solution applied (not illustrated). In the absence of a detectability problem, this result implies that anionic molecules with an MW greater than 500 Da cannot be internalized by pinocytosis.

Discussion

Different types and sizes of vesicles have been demonstrated at the infranuclear [21] and synaptic [33] pole of hair cells using electron microscopy and horseradish peroxidase labeling, respectively. Investigations using the PM marker FM1-43 show that vesicles formed from the reticular lamina transcytose to distinct intracellular compartments that are part of

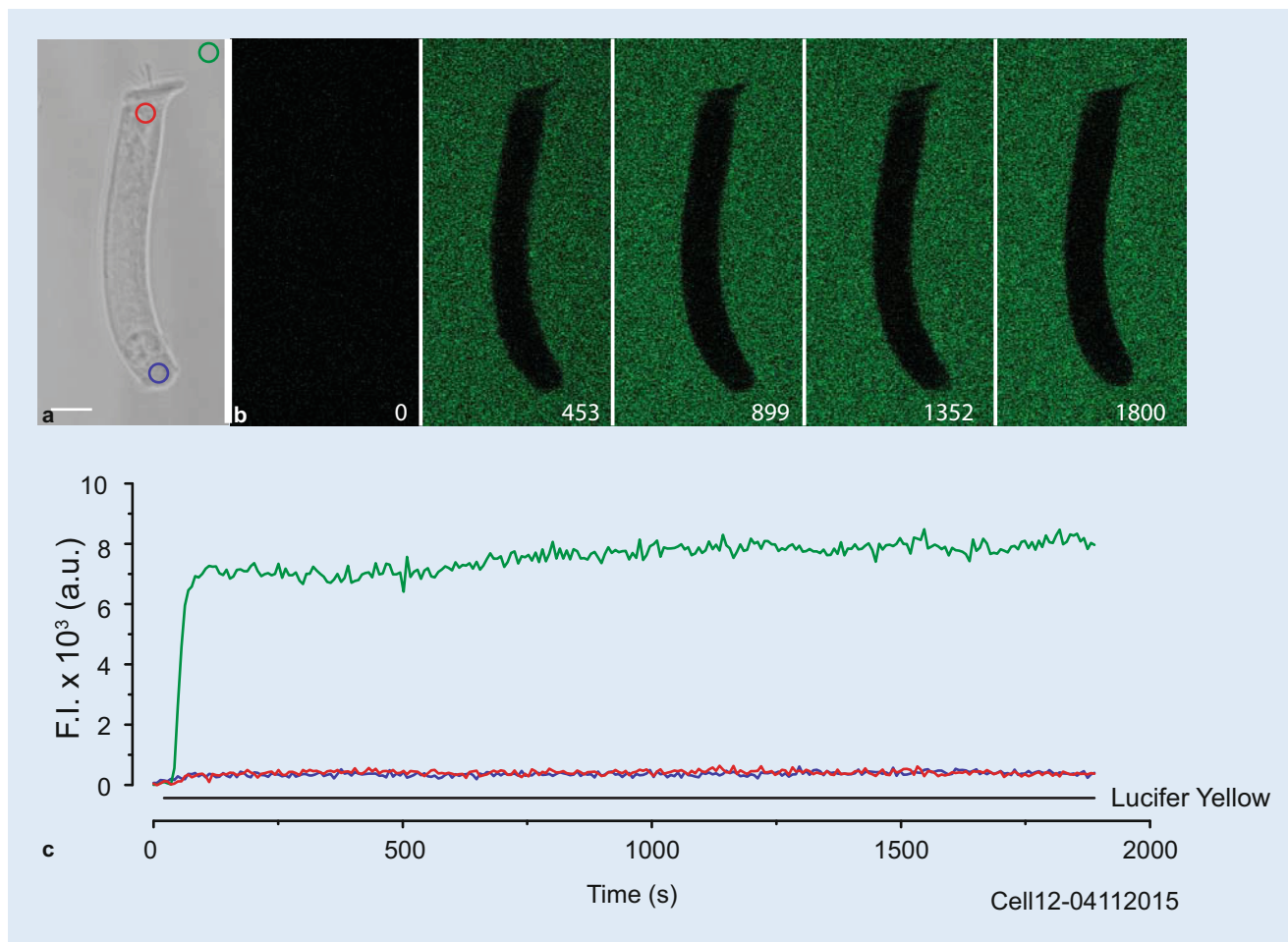


Fig. 4 ▲ Molecular weight limit for uptake by pinocytosis. **a** Phase-contrast image showing intracellular (red and blue circles) and extracellular (green circle) positioned ROIs. Scale bar: 10 μm . **b** Fluorescence images showing Lucifer yellow labeling of extracellular fluid only. Numbers in the bottom right corners indicate experimental time in seconds. **c** Fluorescence signal intensities for the ROIs in panel **a**. Horizontal black line: Lucifer yellow application period

the elaborate endoplasmic reticulum system of the OHC [16, 23]. For isolated bipolar cells such as the OHC, we developed a double-barrel perfusion system to enable the investigation of endocytosis and transcytosis separately from either the apical or the basal pole [18]. Using a pinocytosis and phagocytosis inhibitor, phenylarsine, it was unequivocally demonstrated that the dye uptake is an endocytic process [18]. Furthermore, by incubating the cell in an inhibitor of the motor molecule kinesin, monastrol, we showed that basoapical transcytosis is partially due to a kinesin trafficking mechanism [18].

Here, using the double-barrel perfuser, it was found that endocytosis at the synaptic pole and basoapical trafficking are more intense than endocytosis at

the apical pole and apicobasal trafficking. Double-labeling experiments with DiOC₆ and FM4-64 imply that vesicles internalized at the synaptic pole traffic to the endoplasmic reticulum. The findings are summarized graphically in **Fig. 5**.

Experiments with the low-molecular-weight, fluid-phase endocytic, fluorescent marker Lucifer yellow indicated that pinocytic internalization of anionic molecules is limited to MWs of no more than 500 Da. However, the Lucifer yellow experiments are considered preliminary because if, indeed, there were pinocytic uptake, the number of vesicles might have been insufficient to produce a detectable signal. In these experiments, we limited the concentration of Lucifer yellow (50 μM) to be similar to that used for the PM endocytosis

markers (10 μM). Griesinger et al. (2002) demonstrated pinocytic uptake of Lucifer yellow by inner hair cells for high concentrations (20 mM) and long incubation times (60 min). Future MW experiments should examine the pinocytic uptake of fluorescent markers of much greater extinction coefficient and a higher quantum yield than for Lucifer yellow.

Possible routes of FM1-43 entry into hair cells

It has been shown that FM1-43 can penetrate mechano-electrical transducer (MET) channels in hair cells of immature cochlea cultures [12], hair cells of embryonic mice [13], developing hair and sensory cells [26], cultured chick

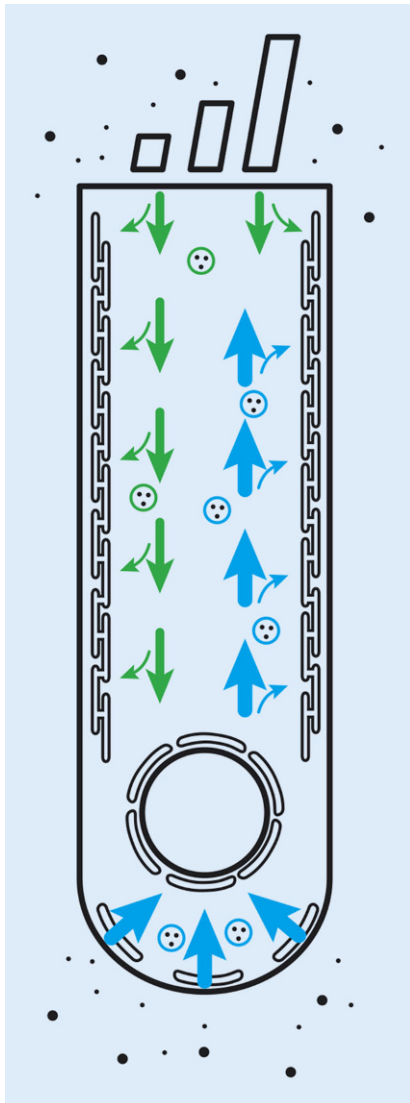


Fig. 5 ▲ Graphical summary. Endocytic activity of the outer hair cell is more pronounced at the synaptic pole and vesicle trafficking is faster toward the apex

auditory papilla hair cells [32], cultured zebrafish larvae lateral line organs [31], and *Xenopus* larvae lateral line organs [28]. In addition, Crumling et al. [5] used hair cells of chicks 5–10 days post-hatch and showed PPADS- and suramin-dependent AM1-43 entry, implying that FM dyes can also penetrate P2X receptors. To avoid this type of nonspecific labeling, recently two techniques were developed: (1) photo-oxidation electron microscopy [22], whereby the FM dye taken up by the organelles is converted to a dark precipitate visible electron microscopically, and (2) instead of us-

ing an FM dye, a novel endocytotic probe impermeable to MET-channels, called membrane-binding fluorophore-cysteine-lysine-palmitoyl group, was used [30]. For both techniques, experiments with IHCs from mice at postnatal day 14–18 yield vastly different patterns of endocytotic signals compared with those found for when uptake is also through the MET channels. Therefore, there is still ongoing controversy about whether FM1-43 does indeed reliably report endocytosis in (P14–18) mice.

However, for the mature cochlea of the guinea pig, there is no evidence of FM1-43 uptake through the MET channels or P2X receptors. For the inner hair cell (IHC), it has been demonstrated, using an in-situ cochlea preparation from young adult guinea pigs, that neither the MET-channel blockers dihydrostreptomycin or D-tubocurarine nor the lesioning of tip links with BAPTA treatment influences FM1-43 labeling [15]. Similar results were reported for OHCs in situ using the same animal and preparation as in the IHC study; namely, that FM1-43 labeling was not influenced by these MET-channel blockers or BAPTA [16]. By applying FM1-43 to isolated OHCs from the mature, pigmented guinea pig cochlea, we also demonstrated that block of MET channels by dihydrostreptomycin or of P2X receptors by PPADS had no influence on the FM1-43 labeling [23]. Therefore, for the experimental model on which the present results are based, there is no evidence of FM1-43 entering through MET channels or P2X receptors of hair cells of the functionally mature cochlea. In other words, the available evidence convincingly suggests that in the present experiments FM1-43 uptake was via endocytic activity.

Physiological relevance of endocytosis in OHCs

Plasma-membrane Ca^{2+} ATPase (PMCA) activity is crucial for removing Ca^{2+} from the cytosol of the stereocilia and, therefore, for protecting hair cells from Ca^{2+} overload [4]. It has been proposed that apical endocytic activity of hair cells is

involved in recycling of PMCA molecules of the hair bundle [14].

Receptors and ion channels of the efferents and afferents located at the synaptic pole of the OHC may require continuous replacement. However, the colocalization data with DiOC₆ and FM4-64 show that vesicles formed at the synaptic pole of OHCs traffic basoapically, targeting the endoplasmic reticulum. Therefore, in addition to PM recycling, proteins such as acetylcholine receptors might also be involved.

It has been proposed that aminoglycoside uptake might be regulated by endocytosis [7]. Although it has been suggested that aminoglycosides enter hair cells through transducer channels in cultured organs from newborn rats [1], the significance of endocytosis-dependent aminoglycoside uptake at the synaptic pole cannot be excluded because aminoglycosides such as gentamicin have a relatively low MW (450–478 Da), which is below the MW limit suggested in this study for pinocytotic internalization. With the aid of the double-barrel perfusor, experiments with fluorescent-labeled gentamicin could address the possibility of its endocytic internalization.

Practical conclusion

- Fluorescent membrane markers enable the investigation of the dynamics of endocytic activity and vesicle trafficking in outer hair cells.
- Such investigations are essential for characterizing cellular mechanisms required not only for membrane and for protein recycling but also for intra- and intercellular communication.
- Mechanisms of vesicle formation and the cargo-specific targets are still debated for outer hair cells.
- Using a recently designed local-perfusion system, the current study demonstrates that basal endocytosis and basoapical trafficking are more intense than apical endocytosis and apicobasal trafficking.
- When coupled with molecular and pharmacological investigations of uptake and trafficking mechanisms, this finding should offer insight into

Abbreviations

A	Apical
AU	Airy unit
a.u.	Arbitrary units
ChA	Channel A
ChB	Channel B
Da	Dalton
DiOC ₆	3,3'-Dihexyloxycarbocyanine iodide
DMSO	Dimethyl sulfoxide
FM1-43	N-(3-Triethylammoniumpropyl)-4-(4-(dibutylamino)styryl)pyridinium dibromide
FM4-64	N-(3-Triethylammoniumpropyl)-4-(6-(4-(diethylamino)phenyl)hexatrienyl)pyridinium dibromide
HBSS	Hanks' balanced salt solution
HEPES	N-2-Hydroxyethylpiperazine-N'-2-ethanesulfonic acid
IC	Infracuticular
IHC	Inner hair cell
IN	Infranuclear
Lucifer yellow	Dipotassium salt of Lucifer yellow carbohydrazide
M	Middle
MET	Mechanoelectrical transducer
MW	Molecular weight
OHC	Outer hair cell
PM	Plasma membrane
PPADS	Pyridoxal phosphate-6-azo(benzene-2,4-disulfonic acid)
ROI	Region of interest
SN	Supranuclear

underlying cellular mechanisms, which is a prerequisite for designing cell-specific medication for hair cells in the future.

Corresponding address



Prof. Dr. A. W. Gummer

Section of Physiological Acoustics and Communication, Faculty of Medicine, Eberhard Karls University Tübingen
Elfriede-Aulhorn-Str. 5,
72076 Tübingen, Germany
anthony.gummer@uni-tuebingen.de

Funding. This work was supported by the Deutsche Forschungsgemeinschaft (DFG), grant Gu 194/9-1, 2.

Compliance with ethical guidelines

Conflict of interest C. Harasztosi and A. W. Gummer declare that they have no competing interests.

The study was approved by the Animal Protection, Veterinary Service and Veterinary Medicine Department of the University of Tübingen and by the Regional Council Tübingen.

Open Access. This article is distributed under the terms of the Creative Commons Attribution 4.0 International License (<http://creativecommons.org/licenses/by/4.0/>), which permits unrestricted use, distribution, and reproduction in any medium, provided you give appropriate credit to the original author(s) and the source, provide a link to the Creative Commons license, and indicate if changes were made.

References

- Alharazneh A, Luk L, Huth M et al (2011) Functional hair cell mechanotransducer channels are required for aminoglycoside ototoxicity. *PLoS ONE* 6:e22347
- Ashmore J (2008) Cochlear outer hair cell motility. *Physiol Rev* 88:173–210
- Betz WJ, Bewick GS (1992) Optical analysis of synaptic vesicle recycling at the frog neuromuscular junction. *Science* 255:200–203
- Beurg M, Nam JH, Chen Q et al (2010) Calcium balance and mechanotransduction in rat cochlear hair cells. *J Neurophysiol* 104:18–34
- Crumling MA, Tong M, Aschenbach KL et al (2009) P2X antagonists inhibit styryl dye entry into hair cells. *Neuroscience* 161:1144–1153
- Dallos P (2008) Cochlear amplification, outer hair cells and prestin. *Curr Opin Neurobiol* 18:370–376
- De Groot JC, Meeuwssen F, Ruizendaal WE et al (1990) Ultrastructural localization of gentamicin in the cochlea. *Hear Res* 50:35–42
- Dong W, Olson ES (2013) Detection of cochlear amplification and its activation. *Biophys J* 105:1067–1078
- Fettiplace R (2017) Hair cell transduction, tuning, and synaptic transmission in the mammalian cochlea. *Compr Physiol* 7:1197–1227
- Frank G, Hemmert W, Gummer AW (1999) Limiting dynamics of high-frequency electromechanical transduction of outer hair cells. *Proc Natl Acad Sci USA* 96:4420–4425
- Froud KE, Wong ACY, Cederholm JME et al (2015) Type II spiral ganglion afferent neurons drive medial olivocochlear reflex suppression of the cochlear amplifier. *Nat Commun* 6:7115
- Gale JE, Marcotti W, Kennedy HJ et al (2001) FM1-43 dye behaves as a permeant blocker of the hair-cell mechanotransducer channel. *J Neurosci* 21:7013–7025
- Géléoc GSG, Holt JR (2003) Developmental acquisition of sensory transduction in hair cells of the mouse inner ear. *Nat Neurosci* 6:1019–1020
- Grati M, Schneider ME, Lipkow K et al (2006) Rapid turnover of stereocilia membrane proteins: evidence from the trafficking and mobility of plasma membrane Ca²⁺-ATPase 2. *J Neurosci* 26:6386–6395
- Griesinger CB, Richards CD, Ashmore JF (2002) FM1-43 reveals membrane recycling in adult inner hair cells of the mammalian cochlea. *J Neurosci* 22:3939–3952
- Griesinger CB, Richards CD, Ashmore JF (2004) Apical endocytosis in outer hair cells of the mammalian cochlea. *Eur J Neurosci* 20:41–50
- Guinan JJ Jr. (2018) Olivocochlear efferents: Their action, effects, measurement and uses, and the impact of the new conception of cochlear mechanical responses. *Hear Res* 362:38–47
- Harasztosi C, Klenske E, Badum S et al (2018) Double fluorescent labelling of a bipolar epithelial cell in vitro: the outer hair cell. *J Neurosci Methods* 293:310–320
- Huang G, Santos-Sacchi J (1993) Mapping the distribution of the outer hair cell motility voltage sensor by electrical amputation. *Biophys J* 65:2228–2236
- Hudspeth AJ (2008) Making an effort to listen: mechanical amplification in the ear. *Neuron* 59:530–545
- Kachar B, Battaglia A, Fex J (1997) Compartmentalized vesicular traffic around the hair cell cuticular plate. *Hear Res* 107:102–112
- Kamin D, Revelo NH, Rizzoli SO (2014) FM dye photo-oxidation as a tool for monitoring membrane recycling in inner hair cells. *PLoS ONE* 9:e88353
- Kaneko T, Harasztosi C, Mack AF et al (2006) Membrane traffic in outer hair cells of the adult mammalian cochlea. *Eur J Neurosci* 23:2712–2722
- Koning AJ, Lum PY, Williams JM, Wright R (1993) DiOC₆ staining reveals organelle structure and dynamics in living yeast cells. *Cell Motil Cytoskeleton* 25:111–128
- Meyer J, Mack AF, Gummer AW (2001) Pronounced infracuticular endocytosis in mammalian outer hair cells. *Hear Res* 161:10–22
- Meyers JR, MacDonald RB, Duggan A et al (2003) Lighting up the senses: FM1-43 loading of sensory cells through nonselective ion channels. *J Neurosci* 23:4054–4065
- Nadol JB Jr. (1983) Serial section reconstruction of the neural poles of hair cells in the human organ of Corti. II. Outer hair cells. *Laryngoscope* 93:780–791
- Nishikawa S, Sasaki F (1996) Internalization of styryl dye FM1-43 in the hair cells of lateral line organs in *Xenopus* larvae. *J Histochem Cytochem* 44:733–741
- Plontke S, Salt AN (2018) Local drug delivery to the inner ear: principles, practice, and future challenges. *Hear Res* 368:1–2
- Revelo NH, Kamin D, Truckenbrodt S et al (2014) A new probe for super-resolution imaging of membranes elucidates trafficking pathways. *J Cell Biol* 205:591–606

31. Seiler C, Nicolson T (1999) Defective calmodulin-dependent rapid apical endocytosis in zebrafish sensory hair cell mutants. *J Neurobiol* 41:424–434
32. Si F, Brodie H, Gillespie PG et al (2003) Developmental assembly of transduction apparatus in chick basilar papilla. *J Neurosci* 23:10815–10826
33. Siegel JH, Brownell WE (1986) Synaptic and Golgi membrane recycling in cochlear hair cells. *J Neurocytol* 15:311–328
34. Terasaki M (1988) Fluorescent labeling of endoplasmic reticulum. *Methods Cell Biol* 29:125–135
35. Zheng J, Shen W, He DZ et al (2000) Prestin is the motor protein of cochlear outer hair cells. *Nature* 405:149–155

Folgenreiche Fake News: Beispiel HPV-Impfung in Japan

Die Behandlung von Patienten auf Basis einer evidenzbasierten Medizin sollte die Richtschnur ärztlichen Handelns sein. Doch was passiert, wenn seriöse Medizinfos übertönt werden von zweifelhaften Erkenntnissen? Ein Fall aus Japan zeigt die Folgen.

In Deutschland rühren verschiedene Ärzteverbände die Werbetrommel, um die Impfraten gegen Humane Papillomviren (HPV) zu steigern – nur knapp die Hälfte der Zielgruppe genießt diesen Impfschutz bereits, obwohl die Evidenzlage klar ist. Japan hingegen verzeichnete 2013 bereits eine Quote von 70 %. Die Impfrate ist aber schlagartig auf das niedrige Niveau von rund 1 % gefallen. Für die japanische Ärztin Riko Muranaka ist die plötzliche Ablehnung der HPV-Impfung vor allem auf eines zurückzuführen: Fake Science und Fake News.

Kehrtwende nach Erfolgsstory

Nachdem die HPV-Impfung unter jungen Mädchen rasant zur Erfolgsstory geworden war, seien plötzlich Schlagzeilen in den Medien aufgetaucht, die den Impfgegnern das Wort redeten – untermauert mit Videos von Mädchen, die behaupteten, geschädigt worden zu sein. Ursache für das plötzliche Medieninteresse seien wissenschaftlich nicht haltbare Studien gewesen – allerdings interessierte sich offenbar niemand für deren Evidenz, führte die Ärztin aus.

Eine Maus sorgt für viel Aufregung

Im Jahr 2016 fand Muranaka eigenen Angaben zufolge dann heraus, dass Dr. Shuichi Ikeda, der auf allen Fernsehkanälen mit seiner Maus-Studie präsent war, die vor der HPV-Impfung warnen sollte, massive wissenschaftliche Defizite aufgewiesen habe. Unter anderem habe Ikeda für seine Studie nur eine einzige Maus benutzt, deren Gehirn durch den Impfstoff geschädigt worden sei. Die Studie sei zudem nie am Menschen repliziert worden.

Sammelklage von über 200 Frauen

Aktuell sehe sich die japanische Regierung einer Sammelklage im Namen von über 200 Frauen ausgesetzt, deren Anwälte sie als Opfer der HPV-Impfung darstellen. Muranaka erwartet eine Prozessdauer von rund 10 Jahren und rechnet in dieser Zeit mit mehreren tausend Toten wegen unterlassener HPV-Impfung.

Staatliche Empfehlung abgeschwächt

Die Regierung stehe unter Feuer, weil es ursprünglich eine staatliche Empfehlung für die Impfung gegeben habe, die inzwischen abgeschwächt worden sei. Es wird lange dauern, bis sich die HPV-Impfrate wieder erholen kann, so Muranaka. Aus ihrer Sicht liegt ein erheblicher Teil der Verantwortung bei den Medien: „Die Medien berichten immer noch eher auf Basis von Emotionen als von wissenschaftlichen Fakten.“

Nährboden für Impfgegner

Sie habe den Eindruck, dass die japanische Medienlandschaft nicht so vielfältig sei wie in anderen Ländern, erläuterte sie. Der Erfolg der Impfung war nach ihrer Einschätzung mit verantwortlich, dass die Botschaften der Impfkritiker auf fruchtbaren Boden fallen konnten. In der Folge seien die entsprechenden Infektionen kaum noch sichtbar gewesen, das Problembewusstsein sei entsprechend gesunken.

**Quelle: Ärzte Zeitung
www.aerztezeitung.de**